Application of a Transition Transport Model to Industrially Relevant Aerodynamic Configurations

Cornelia Seyfert
Deutsches Zentrum für Luft- und Raumfahrt - DLR (German Aerospace Center), Institute of Aerodynamics and Flow Technology, C²A²S²E Center for Computer Applications in AeroSpace Science and Engineering,
Bunsenstraße 10, 37073 Göttingen, Germany,
cornelia.seyfert@dlr.de.

The correlation-based γ-$Re_{\theta t}$ transition transport model has been implemented into a hybrid Reynolds-Averaged Navier-Stokes solver and evaluated on various basic test cases. The present work deals with the application of the γ-$Re_{\theta t}$ transition transport model to more complex and industrially relevant aerodynamic configurations. Results are shown for the computation of flow around a 2D high-lift airfoil and a 3D helicopter fuselage. The computed transition locations as well as the pressure and skin friction coefficient distributions are presented. The influence of the model specific parameters, the turbulence intensity and the turbulent to molecular viscosity ratio on the resulting transition locations is investigated. Modifications were applied to the original γ-$Re_{\theta t}$ transition model and the arising differences between the results are discussed.

I. Introduction

Within the past years parallel computation capacities increased enormously and physical models which exhibit flexible parallelization performance for fluid dynamic computations become more and more important. On future architectures, the parallelization efficiency of physical models will play a even more significant role.
The characterization of flows around wings, fuselages and airfoils includes the modelling of laminar to turbulent transition in the boundary layer. The prediction of boundary layer transition is an important component in the computation of flows over airfoils and wings because flow quantities like friction or drag coefficients are affected by the transition process. For aerodynamic flow configurations the e^N-method is the most established way to predict transition [1,2]. As the e^N-method is a streamline based approach, its parallelization efficiency and integration level into a Reynolds-Averaged Navier-Stokes (RANS) code is limited, which paves the way for investigation of alternative transition prediction approaches. The local correlation-based γ-$Re_{\theta t}$ transition transport model was developed and published by F. Menter and R. Langtry since 2004 [3-5]. The idea behind is to predict transition using local variables, which enables its implementation into a RANS framework and affords the same degree of parallelization as other transport equations models.
The γ-$Re_{\theta t}$ transition transport model holds two transport equations. The transport equation for the intermittency γ triggers transition inside the boundary layer. Its production term is mainly induced by the turbulent to molecular viscosity ratio and the model specific local to non-local Reynolds number correlation. The intermittency is coupled to the production and destruction terms of the turbulent kinetic energy k. The associated turbulence model is the SST k-ω turbulence model of Menter [6]. The second equation transports the Reynolds number based on momentum thickness at transition onset $Re_{\theta t}$. Its source term is controlled by an empirical transition criterion which is a function of the local turbulence intensity and the stream wise pressure gradient. An implemented boundary layer detector ensures the transport of $Re_{\theta t}$ in the freestream up to the boundary layer edge. The γ-$Re_{\theta t}$ transition transport model is based on a 2D model of the boundary layer which allows for prediction of 2D transition phenomena, but does not account for 3D transition mechanisms such as crossflow instability.
The γ-$Re_{\theta t}$ transition transport model has been implemented into the hybrid, three-dimensional, parallelized RANS based DLR TAU code [7-9]. Basic investigation and validation was performed for a flat plate test case and for certain one element airfoils such as the AS-A, AS-B and Somers NLF airfoil [10]. Different approaches for model relevant empirical functions and various transition criteria have been analyzed. The results were compared and evaluated with experimental data and results obtained by the standard transition prediction approach in TAU, the e^N-method. Further analysis of the transition transport model has been carried out on a 2D Messerschmidt-Bölkow-Blohm airfoil [11].

The sensitivity of the γ-$Re_{\theta t}$ transition transport model related to the boundary conditions for the turbulence intensity $Tu_{\infty,init}$ and the ratio of turbulent to molecular viscosity $\mu_T/\mu|_{init}$ is shown for the given case.
The present work deals with the application of the γ-$Re_{\theta t}$ model to industrially relevant aerodynamic configurations. The test cases selected, represent two different aerodynamic flows. First, the computational results for the flow around the three-element airfoil of the A310 in take-off configuration are shown. This is a high-lift test case, which has been extensively investigated both numerically [12] and experimentally [13]. For the slat and the flap experimentally determined transition locations are available. These transition locations were compared to the transition locations obtained with the γ-$Re_{\theta t}$ transition transport model. Additionally, the results are compared to those of the standard transition prediction method in TAU based on the e^N-method.
The second test case is the fuselage of a helicopter. Here, data from an estimation of the transition locations are available. The numerical investigation of flow around the helicopter fuselage was part of an European research project [14]. Application of the γ-$Re_{\theta t}$ model to the flow around the helicopter yields reasonable results for the transition locations.

II. Three-element airfoil A310 in take-off configuration

The three-element airfoil of the A310 was part of a comprehensive experimental study within the Garteur High Lift Action Group. The measurements were performed in the ONERA F1 wind tunnel. Various Mach and Reynolds numbers as well as different angles of attack were considered. The flows over take-off and landing configuration of the airfoil were investigated.
For the results given here, the following parameters were used: $M = 0.22$, $Re \approx 6.0$ Mio. The angle of attack was set to $\alpha = 21.4°$. In the experiments, the transition locations were determined on the upper side of the airfoil elements. On the slat, the transition location is at $x/c|_{tr,flap} = 0.15$ and on the flap it is at $x/c|_{tr,slat} = 0.35$. On the main wing, transition was not measured, but the surface holds a discontinuity which is the point where the trailing edge of the slat is located in case of the undeflected configuration. The discontinuity may trigger transition on the upper side of the main wing and serves as an orientation point. It is located at $x/c|_{unst,main} = 0.19$. Transition was not measured on the lower side of the airfoil.
For the computations, two different unstructured grids [12] were used. The coarse grid consists of 22.000 primary grid points, while the second grid contains 122.000 grid points. For the fine grid, the resolution inside the boundary layer has been highly increased. For the coarse grid around 50 prism layers were located next to the surface of the airfoil, while for the fine grid around 100 prism layers were used. Also parallel to the wall the element number was increased for the fine grid. The flow on the fine grid results in a $y^+(1)|_{max} \approx 2$ for the cell next to the wall, while on the coarse grid $y^+(1)|_{max} \approx 4$ is obtained. In the laminar flow region $y^+(1)$ for the fine grid is smaller than 1, while on the coarse grid it is in the range of 3 to 4. Figure 1 shows the two grids for the A310 in take-off configuration.

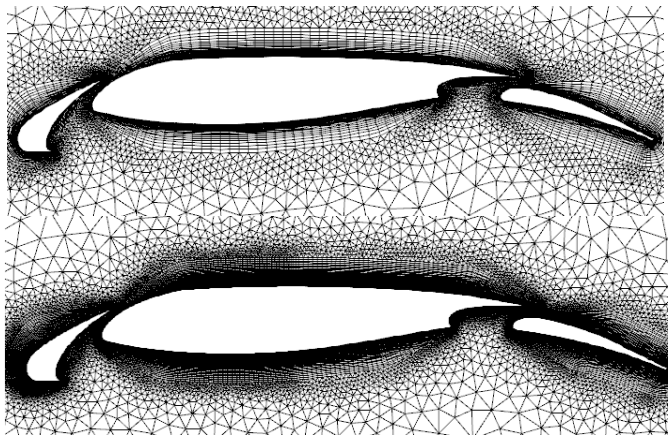

Figure 1. Coarse and fine grid for the A310 in take-off configuration

All the computations were performed with the DLR TAU Code in RANS mode. The Menter SST k-ω turbulence model has been used in combination with the γ-$Re_{\theta t}$ transition transport model. For the empirical functions the model makes use of the standard formulation given by Menter and Langtry [5]. The same holds for the transition criterion. As TAU is a compressible solver and the Mach number for the given case was moderate, preconditioning was turned on for the computations. This will improve the prediction of the aerodynamic coefficients, but leads to worse convergence quality. However, sufficient convergence was obtained.

The turbulence intensity is an important input parameter for the γ-$Re_{\theta t}$ transition transport model and affects the prediction of the transition locations significantly. A realistic guess for the turbulence intensity in the vicinity of the airfoil and at the boundaries of the geometry is important. The application of the two-equation turbulence models goes along with a decay of turbulence in the freestream. When setting the turbulence intensity at the farfield boundary, this decay has to be considered. For the present case the decay is not critical because of the low freestream turbulence level of $Tu_\infty \approx 0.07\%$. The initial value at the farfield boundary was set to $Tu_{\infty,init} = 0.08\%$.

The second input parameter for the γ-$Re_{\theta t}$ transition transport model is the turbulent to molecular viscosity ratio. This ratio will trigger the production of the intermittency in the boundary layer and is also part of the production term within the $Re_{\theta t}$ equation. Furthermore, it affects the decay of the turbulence intensity in the freestream. For the flow around one-element airfoils, the ratio is set to values in the order of 1 - 10. This ensures the presence of turbulence within the flow in the vicinity of the airfoil. For the three-element airfoil the situation is different. Caused by the flow over the slat and the main wing, turbulence is produced inside the flow field and a high initial viscosity ratio may result into upstream movement of transition locations on the main wing and the flap. To investigate the influence of the initial viscosity ratio on the transition locations, a variation of the parameter was done and the results are discussed.

First, the distributions of the pressure coefficient are considered. Experimentally determined pressure coefficients are compared to results of transitional computations on both grids and to results obtained by a fully turbulent computation. The left hand side of figure 2 shows the pressure coefficient as a function of the chord length for the three airfoil elements.

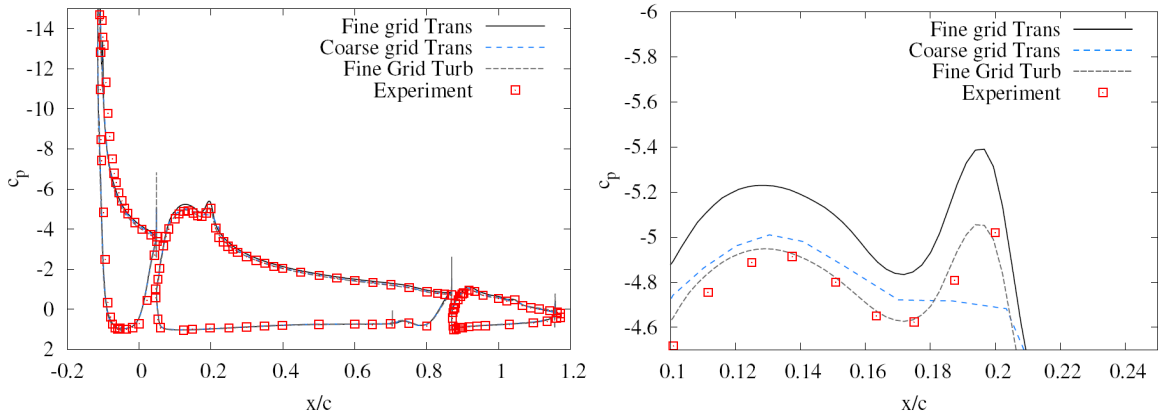

Figure 2. Pressure coefficient distribution for slat, main wing and flap (left) and an enlarged representation of the suction peak on the main wing (right)

On both grids, the results of turbulent and transitional computations are in good agreement with the experimental data. On the right hand side of figure 2, the suction peak on the main wing is displayed. For the flow computation on the coarse grid, the characteristic of the distribution is poorly represented, while computation on the fine grid displays the trend correctly. The results of the fully turbulent computation are closer to the experimental data.

In figure 3 the skin friction distributions are plotted for computations with different initial viscosity ratios for the γ-$Re_{\theta t}$ transition transport model. The initial turbulence intensity $Tu_{\infty,init}$ was not changed. All computations were performed on the fine grid. For comparison also the measured transition locations are plotted.

On the upper side of the slat c_f is small for an initial viscosity ratio of $\mu_T/\mu|_{init} = 0.01$ and close to the result of the fully turbulent computation. Transition is induced by laminar separation on the slat for all computations. For $\mu_T/\mu|_{init} = 0.01$ the transition location is at $x/c|_{tr,slat} = 0.11$ and for $\mu_T/\mu|_{init} = 1.0$ the

transition location is at $x/c|_{tr,slat} = 0.09$. The transition locations for the application of the γ-$Re_{\theta t}$ transition transport model are defined by the distribution of the intermittency in the boundary layer. If the intermittency increases from $\gamma = 0$ to 1, the transition location is determined at $\gamma \approx 0.5$.

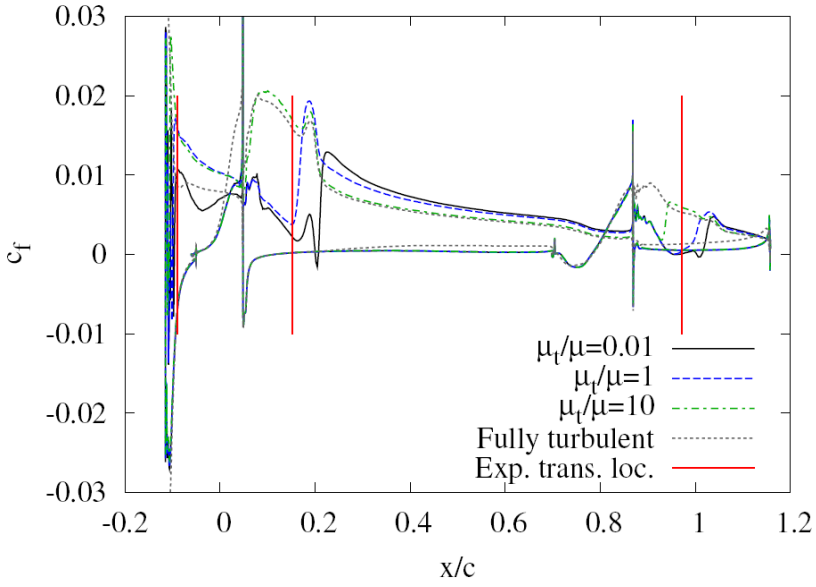

Figure 3. Skin friction coefficient distributions for transitional and turbulent flow computations

On the upper side of the main wing, the distribution of c_f for $\mu_T/\mu|_{init} = 10$ is almost the same as for the fully turbulent computation. The high initial viscosity ratio causes increased turbulence intensity in the vicinity of the airfoil elements. The intermittency production is activated upstream compared to the computations with lower initial viscosity ratios. For decreasing initial viscosity ratios the transition locations move downstream and the skin friction distributions show laminar regions. While transition is still induced upstream of the discontinuity on the main wing for $\mu_T/\mu|_{init} = 1$, the transition location for $\mu_T/\mu|_{init} = 0.01$ is slightly downstream this point.
The increase of the skin friction coefficient distribution for $\mu_T/\mu|_{init} = 0.01$ close to $x/c = 0.2$ can be traced back to the discontinuity. But the transition is delayed and a small separation occurs downstream the discontinuity. The position of transition is at $x/c|_{tr,main} = 0.08$ for $\mu_T/\mu|_{init} = 1$ and at $x/c|_{tr,main} = 0.16$ for $\mu_T/\mu|_{init} = 0.01$.
On the upper side of the flap transition occurs still upstream of the measured transition location for an initial viscosity ratio of $\mu_T/\mu|_{init} = 10$. For reduced initial viscosity ratios transition is predicted downstream of experimental data, which was not the case for transition prediction on the slat and on the main wing. The reason for this might be the magnitude of transported turbulence in the wake of the main wing. The boundary layer on the flap is not sufficiently influenced by the turbulence. This leads to a downstream movement of the transition location for low initial viscosity ratios. An initial viscosity ratio of $\mu_T/\mu|_{init} = 0.01$ leads to a transition location on the flap of $x/c|_{tr,flap} = 0.52$, while an initial viscosity ratio of $\mu_T/\mu|_{init} = 1$ causes transition at $x/c|_{tr,flap} = 0.43$.
Considering the minimum of the skin friction coefficient distribution as the transition point, an initial viscosity ratio of $\mu_T/\mu|_{init} = 1$ leads to excellent agreement of computed and measured transition locations.
Figure 4 shows the comparison of results obtained by the γ-$Re_{\theta t}$ transition transport model and by the e^N-method. For the latter, the RANS solver TAU is coupled to an external boundary-layer code and a local linear stability code. Again, the Menter SST k-ω turbulence model is used for the computation. On the slat the c_f distribution for the e^N-method is close to the computational results of the γ-$Re_{\theta t}$ model with $\mu_T/\mu|_{init} = 1$. An influence of the discontinuity is visible on the main wing, but no separation appears. Transition locations are comparable to those of the γ-$Re_{\theta t}$ transition transport model with $\mu_T/\mu|_{init} = 0.01$. On the flap, transition is close to the transition location obtained with $\mu_T/\mu|_{init} = 10$, which is at $x/c|_{tr,flap} = 0.22$. In contrast to the γ-$Re_{\theta t}$ model, the magnitude of the local turbulence quantities computed by the RANS solver is not directly influencing the transition prediction for the e^N-method. The linear stability analysis is done by means of superimposing artificially generated waves.

The transition locations computed with the γ-$Re_{\theta t}$ transition transport model for an initial viscosity ratio of $\mu_T/\mu|_{init} = 0.01$ are in good agreement with the experimental data for the slat and the main wing. For the flap transition appears too far downstream. Setting the initial viscosity ratio to $\mu_T/\mu|_{init} = 1$ leads to upstream transition locations on the slat and especially on the main wing but to an improved transition prediction on the flap.

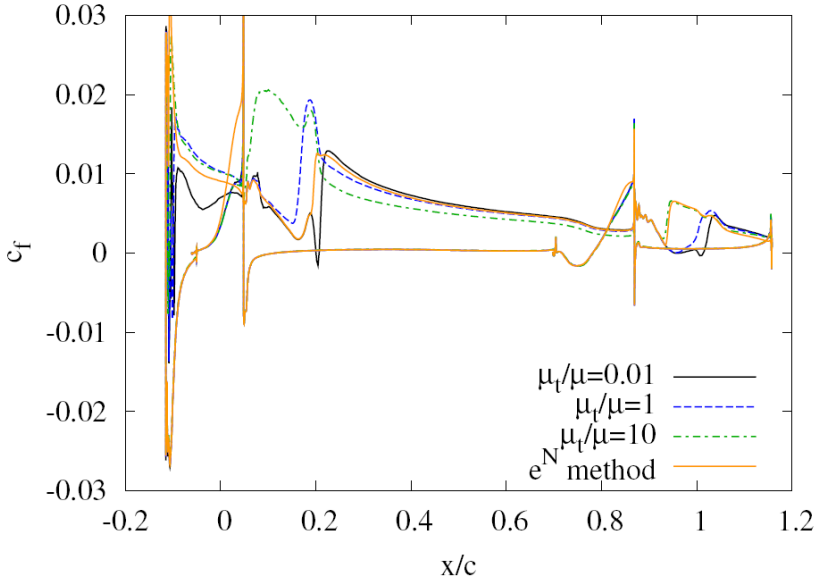

Figure 4 Skin friction coefficient distributions for different transition prediction approaches

In order to investigate the influence of the local turbulence quantities on the transition prediction further, a modification of the γ-$Re_{\theta t}$ transition transport model is applied. The transport equation for $Re_{\theta t}$ is no longer used, and the local evaluation of the transition criterion is removed. Instead the transition criterion is evaluated with the initial freestream turbulence intensity. A fixed critical $Re_{\theta t,crit}$ is obtained which is used for the evaluation of the intermittency transport equation. This will decouple the model from local turbulence intensity. The computational effort is reduced, because only one transport equation is solved. The model constants and empirical functions were not changed.

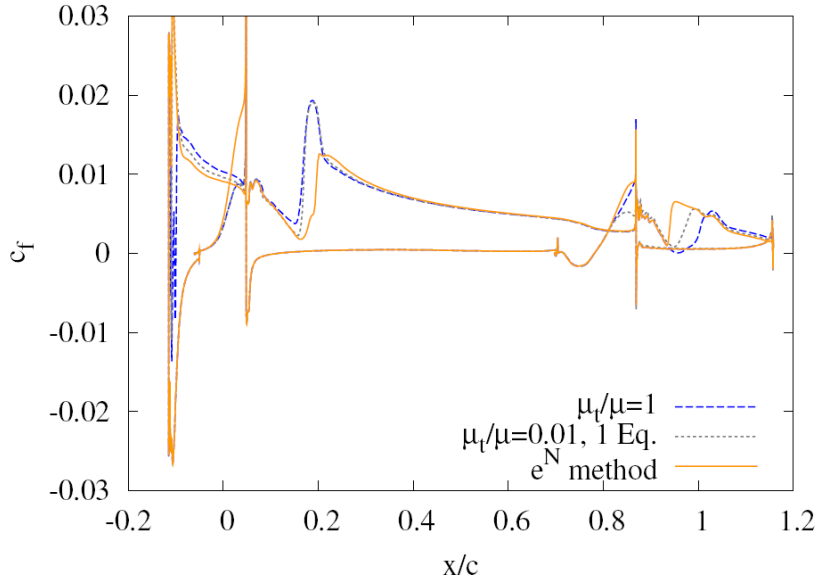

Figure 5. Skin friction distribution for the modified transition model

Figure 5 shows the result for the skin friction coefficient distribution. An initial turbulence intensity of $Tu_{\infty,init} = 0.08\%$ and an initial viscosity ratio of $\mu_T/\mu|_{init} = 0.01$ are set. On the slat and main wing the distribution of c_f is similar to the results of the original model with $\mu_T/\mu|_{init} = 1$. But on the flap transition appears upstream of the transition locations predicted by the original model. The transition location on the main wing is at $x/c|_{tr,main} = 0.15$ and on the flap at $x/c|_{tr,flap} = 0.38$ which is in good agreement with the measured transition location.
The transition locations and the skin friction distribution computed with the modified transition model are closer to the results given by the e^N-method.

III. Helicopter fuselage

Transition on a helicopter fuselage was investigated with the γ-$Re_{\theta t}$ transition transport model. Measured transition locations are not available but an estimation of the transition line exists. The primary grid used for computation consists of hexahedral cells and around 840.000 points. Near the fuselage the grid is refined. For the given flow $y^+(1)$ is smaller than 0.7 in the cell next to the wall for the complete surface.
A fully turbulent simulation with the Menter SST k-ω model was performed for comparison. The flow parameters were M = 0.236, Re = 30 Mio. and the angle of attack was set to $\alpha = 0.016°$.
Figure 6 shows the distribution of c_f on the surface of the helicopter. On the left hand side the result of the fully turbulent simulation is shown, while on the right hand side the transitional flow result is displayed. The skin friction coefficient is plotted in the same range.

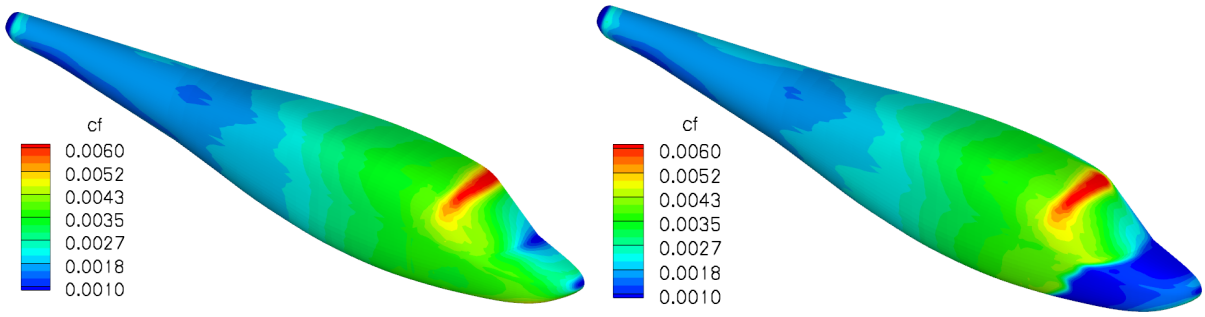

Figure 6. Skin friction distribution on the surface of the helicopter for fully turbulent (left) and transitional (right) flow computation

The initial turbulence intensity for the transitional computation was set to $Tu_{\infty,init} = 1\%$ and the initial viscosity ratio to $\mu_T/\mu|_{init} = 10$. Similar to one-element airfoil computations and in contrast to the three-element airfoil computation the initial viscosity ratio needs to be set to higher values, because no turbulence is produced by the flow. Setting these initial conditions at the farfield boundary, leads to a turbulence intensity in the vicinity of the fuselage of $Tu_\infty \approx 0.07\%$.
Besides the application of the original γ-$Re_{\theta t}$ transition transport model, alternative approaches for some model specific functions were used. The empirical functions for F_{length} and $Re_{\theta c}$ were replaced by functions of Suluksna et al. [14] and a transition criterion of Abu-Ghannam and Shaw [15] was used.
The transition locations on the fuselage for the computations with the γ-$Re_{\theta t}$ transition transport model are obtained by the intermittency distribution inside the boundary layer. If the intermittency increases from $\gamma = 0$ to 1, transition is determined at $\gamma = 0.5$.
Figure 7 shows the transition lines on the helicopter fuselage for the different computations as well as the estimated transition line. The black line represents the estimation ("Estim. TL"), while the orange line shows the result of the original model formulation ("γ-$Re_{\theta t}$ model") and the blue line displays the model with the modified functions ("Mod. γ-$Re_{\theta t}$ model."). The side view on the fuselage shows a deviation of the transition line in some parts between the computations and the estimated transition line. Compared to the fuselage size the difference is less than 5%. In the lower part, the transition locations computed with the modified model functions are downstream compared to the original model and the estimated transition positions. The overall tendency of the distribution of transition locations on the surface is the same for the computations and the estimation.

On the bottom side of the fuselage the transition locations move upstream which is reproduced by the computational results. The gradient and curvature of the transition lines are similar. However, a constant offset is present. For the estimated solution, transition locations are further upstream than the numerically obtained transition locations.
The top side shows excellent agreement of the transition lines for both computations.

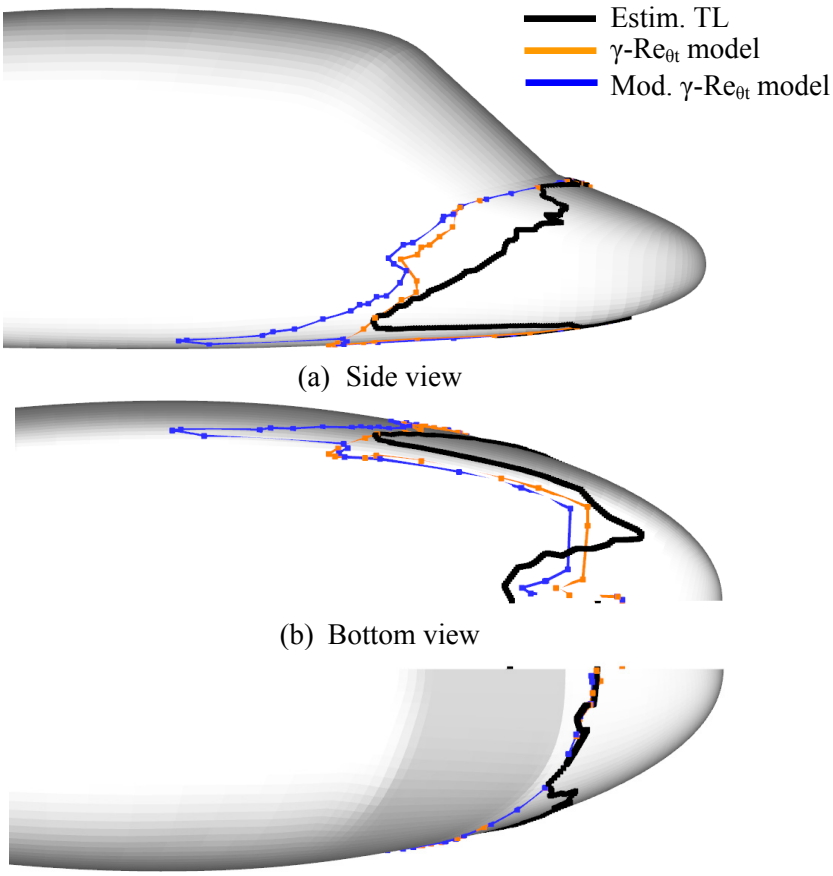

(a) Side view

(b) Bottom view

(c) Top view

Figure 7. Transition lines on the helicopter fuselage.

IV. Conclusion

From the presented results it is shown that the γ-$Re_{\theta t}$ transition transport model can be applied to a complex, industrially relevant high-lift airfoil such as the A310 in take-off configuration. The predicted transition locations are in the range of the experimental data if appropriate initial conditions are set for the γ-$Re_{\theta t}$ transition transport model. The variation of the initial viscosity ratio showed its wide influence on the predicted transition locations.
The transition model was modified by the removal of the transport equation for $Re_{\theta t}$ and by an evaluation of the transition criterion with the initial freestream instead of the local turbulence intensity. Caused by the independence of the local turbulent quantities, the predicted transition locations and c_f distributions differ. Especially on the flap of the three-element airfoil the transition prediction is improved.
The application of the γ-$Re_{\theta t}$ transition transport model to the flow around a helicopter fuselage results in acceptable transition prediction. Although the turbulence quantities were unknown, computations yield reasonable results. The characteristic of the transition line on the surface is very well represented and the skin friction distribution suggests an improvement of prediction of aerodynamic coefficients for the helicopter.
The presented results provide a basis for further application of the γ-$Re_{\theta t}$ transition transport model to complex 2D and 3D configurations. Besides the accuracy of the predicted transition locations, a focus will be set on the investigation of the parallel performance of the model.

References

[1] Krumbein, A., Krimmelbein, N. Schrauf, G., "Automatic Transition Prediction in a Hybrid Flow Solver – Part 1: Methodology and Sensitivities", *Journal of Aircraft*, Vol. 46, No. 4, 2009, pp. 1176-1190.

[2] Krumbein, A., Krimmelbein, N. and Schrauf, G., "Automatic Transition Prediction in a Hybrid Flow Solver – Part 2: Practical Application", *Journal of Aircraft*, Vol. 46, No. 4, 2009, pp. 1191-1199.

[3] Menter, F. R., Langtry, R. B., Likki, S. R., Suzen, Y. B., Huang, P. G. and Völker, S., "A Correlation-Based Transition Modeling Using Local Variables Part 1: Model Formulation" *Journal of Turbomachinery*, Vol. 128, No. 3, 2006, pp. 413-422.

[4] Menter, F. R., Langtry, R. B., Likki, S. R., Suzen, Y. B., Huang, P. G. and Völker, S., "A Correlation-Based Transition Modeling Using Local Variables Part 2: Test Cases and Industrial Applications" *Journal of Turbomachinery*, Vol. 128, No. 3, 2006, pp. 423-434.

[5] Menter, F. R. and Langtry, R. B., "Correlation-Based Transition Modeling for Unstructured Parallelized Computational Fluid Dynamics Codes" *AIAA Journal*, Vol. 47, No. 12, 2009, pp. 2894-2906.

[6] Menter, F. R., "Two-Equation Eddy-Viscosity Turbulence Models for Engineering Applications", *AIAA Journal*, Vol. 32, No. 8, 1994, pp. 1598-1605.

[7] Schwamborn, D., Gerhold, T., and Hannemann, V., "On the validation of the DLR TAU Code", *New Results in Numerical and Experimental Fluid Mechanics II*, *Notes on Numerical Fluid Mechanics*, Vol. 72, Braunschweig, Wiesbaden, Vieweg Verlag, 1999, pp. 426-433.

[8] Kroll, N., Rossow, C.-C., Schwamborn, D., Becker, K. and Heller, G., "MEGAFLOW - A Numerical Flow Simulation Tool for Transport Aircraft Design", *ICAS Congress 2002 [CD-Rom]*, ICAS, Toronto, Canada, 2002, pp. 1.105.1-1.105.20.

[9] Schwamborn, D., Gerhold, T. and Heinrich, R., "The DLR TAU-Code: Recent Applications in Research and Industry", European Conference on Computational Fluid Dynamics, ECCOMAS CFD 2006, Egmond aan Zee, The Netherlands, 5 – 8 September 2006, *ECCOMAS CFD 2006 - CD-Rom Proceedings*, editors: P. Wesseling, E. Oñate, J. Périaux, 2006, ISBN: 90-9020970-0, © TU Delft, The Netherlands.

[10] Seyfert, C., Krumbein, A., "Evaluation of a Correlation-based Transition Model and Comparison with the e^N-method", AIAA-2010-4443, *40th AIAA Fluid Dynamics Conference*, Chicago, USA, 2010.

[11] Seyfert, C., Krumbein, A., "Comparison of a Local Correlation-Based Transition Model with a e^N-Method for Transition Prediction", *17. DGLR-Fach-Symposium der STAB*, Berlin, Germany, 2010.

[12] Krumbein, A., Krimmelbein, N., "Navier-Stokes High-Lift Airfoil Computations with Automatic Transition Prediction Using the DLR TAU Code", *15. DGLR-Fach-Symposium der STAB*, Darmstadt, Germany, 2006.

[13] Manie, F., Piccin, O. and Ray, J.P., "Test Report of the 2D model M1 in the Onera F1 Wind Tunnel", GARTEUR High Lift Action Group AD (AG-08), TP041, October 1989.

[14] HELIFUSE-Helicopter Fuselage Drag, Assessment report, Task 2 - Navier-Stokes Calculations, Assessment of Blind Test Calculations, Deliverable of subtask 2.1, HELIFUSE/C/1/DLR/03/A, 1997.